ISBN: 978-3-95450-184-7 doi:10.18429/JACoW-IPAC2018-THPML070

POINT SPREAD FUNCTION STUDY OF QUASI-MONOCHROMATIC X-RAY PINHOLE CAMERA AT SSRF *

B. Gao[1], Y. B. Leng[1,†], H. J. Chen[1], J. Chen
Shanghai Institute of Applied Physics, Chinese Academy of Sciences, 201800 Shanghai, China
[1]also at University of Chinese Academy of Sciences, 100049 Beijing, China

Abstract

Since 2009 an X-ray pinhole camera has been used to present the transverse beam size and emittance at Shanghai synchrotron radiation facility. However, the performance of the pinhole camera is determined by the width of the point spread function. In order to measure the point spread function more accurately and more conviently, an X-ray quasi-monochromator has been established. Combined with this monochromator, a novel method called variable wavelength based point spread function calibration method. In this article, a simulation study of the point spread function calibration of the new X-ray pinhole camera will be presented in detail.

INTRODUCTION

The emittance at the storage ring of SSRF is 3.9 nm.rad, and the designed transverse beam size, at the source point of the X-ray diagnostic beam line, is 73 μm at horizontal and 22 μm at vertical.

X-ray pinhole cameras are widely used to measure the transverse beam size and emittance around the world [1–4]. An X-ray pinhole camera has been estabished on the diagnostic beam line at Shanghai synchrotron radiation facility (SSRF) [5].

The performance of the pinhole camera is determined by the width of the point spread function (PSF). It is very import to measure or calculate the PSF more accurately and more conveniently. Variable beam size based PSF calibration method was introduced at year of 2012 [6]. By varying the beam size at the source point and measuring image size, the practical value of PSF can be derived. With this, a more accurate resolution for the pinhole camera can be derived. However, this experimental method requires to change the beam size, which is not able to be carried out under user operation mode.

Varible wavelength based PSF calibration method was proposed by SSRF [7]. A quasi-monochromator was installed at the pinhole camera system [7]. Combined with this quasi-monochromator, the new pinhole camera is expected to realize the calibration of PSF under any beam conditions.

We have studied PSF calibration of the new X-ray pinhole camera with the goal of realizing a PSF calibration under any beam conditions. In this article, the simulation study of the novel calibration method will be presented in detail. This study was done using the SRW simulation code [8].

* Work supported by National Science Foundation of China (No.11375255)
† leng@sinap.ac.cn

System Layout

A pinhole camera is installed in the storage ring of SSRF. Its working principle is described in detail in [5]. In new system, an X-ray monochromator has been installed before the screen of the pinhole camera system. The new X-ray pinhole camera is shown as Fig. 2 [7]:

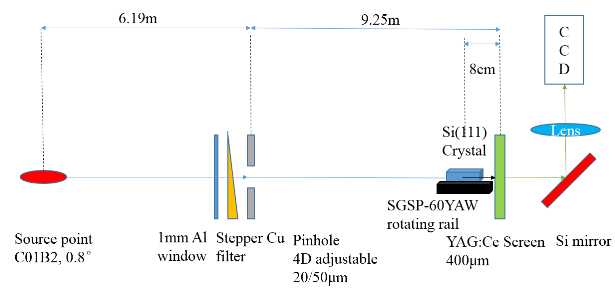

Figure 1: System layout of the new X-ray pinhole camera at SSRF.

In the new pinhole camera, a Si(111) crystal combined with a rotating rail was used as a quasi-monochromator [7]. A crystal monochromator operates through the diffraction process according to Bragg's law. Photon energy (wavelength) can be selected by crystal, net planes, and Bragg angle [9]. Monochromator selection must cover the main energy range of the spectrum. The spectrum of the extracted X-ray photon beam at the X-ray diagnostic beam line is shown as Fig. 2. For Si(111) crystal, when the bragg angle

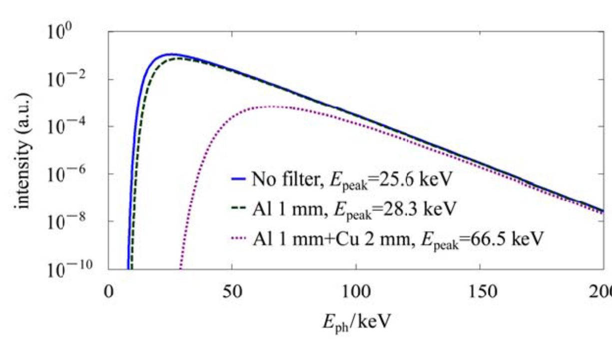

Figure 2: The spectrum of the extracted X-ray photon beam.

changes from 3 deg to 70 deg, the detected energy range is between 2 keV and 40 keV. Hence, the energy range of Si(111) crystal is able to cover the range of the main area of the spectrum of the X-ray photon beam.

ISBN: 978-3-95450-184-7 doi:10.18429/JACoW-IPAC2018-THPML070

SIMPLE THEORETICAL CALCULATION OF PSF

The resolution of an X-ray pinhole camera is determined by its aperture and by the resolution of the imaging system (scintillator, lenses, CCD). For the sake of simplicity, we can add quadratically all widths of the pinhole PSFs. It is an approximation since this is valid only for assumption of Gaussian distributions.

The total measured beam size can be described in Eq. (1):

$$\sigma_{img} = \sqrt{\sigma_{beam} * C_{mag}{}^2 + \sigma_{pinhole}^2 + \sigma_{detector}^2}, \quad (1)$$

Where C_{mag} is the magnification, σ_{beam} is the RMS width of the source spot, $\sigma_{pinhole}$ is the pinhole width of the complete PSFs and $\sigma_{detector}$ is the visible light detector width.

Concerning the pinhole itself, the resolution is determined by both the diffraction and geometrical projection of the pinhole opening. A small aperture will lead to diffraction and a large aperture will lead to image blurring by the geometrical projection of the pinhole opening. $\sigma_{pinhole}$ is described as follows:

$$\sigma_{pinhole} = \sqrt{\sigma_{diff}^2 + \sigma_{aper}^2}, \quad (2)$$

For the diffraction part, its RMS width can be calculated from:

$$\sigma_{diff} = \frac{\sqrt{12}\lambda D}{4\pi A}, \quad (3)$$

Where λ is the X-ray wavelength, D is the distance from pinhole to the scintillator, A is the hole width. This formula shows that the diffraction improving with larger holes.

However, for large holes the PSF is dominated by the geometrical projection. For the pinhole camera, a point source of light illumination a rectangular hole at a distance d, will project a spot of light on the scintillator. The size of the spot is A(D+d)/d, where d is the distance from source point to the pinhole. The corresponding RMS width of the geometrical projection is:

$$\sigma_{aper} = \frac{A(D+d)}{\sqrt{12}d} \quad (4)$$

The complete PSF also contains the imaging system widths. The PSF of the imaging system including the screen, mirror, lens and the CCD camera. The problem is that this part of PSFs is hard to calculate, a calibration experiment has been discussed at [10].

VARIABLE WAVELENGTH BASED PSF CALIBRATION

Simple theoretical calculation of PSF is discussed in the previous section. In this section the novel calibration method will be discussed.

According to Eq. (1), the total measured beam size contains several parts. For the same pinhole system, the pinhole and imaging system widths of the PSFs are constant.

By changing the beam size of the source spot and observing the total measured beam size, the PSF is able to be derived. This variable beam sizes based calibration method has been discussed in [6]. However, this calibration method requires to change the beam size which is not able to be carried out under any beam conditions. In this article a novel variable wavelength based calibration method will be discussed.

Assume the beam size of the source point is constant, the image size can be obtained from the CCD camera. Since the pinhole and the imaging system is same, so the geometric and imaging system widths of PSFs are constant. The diffraction width is determined by the wavelength. Since synchrotron radiation extracted from the bending magnet is emitted with a wide range of energies. If the wavelength of the X-ray can be changed, the PSF of pinhole is also able to be derived.

The principle of the variable wavelength based PSF calibration method is by selecting different wavelength of the X-ray, and observing the change of the imaging spot size. This is under the assumption of the beam size is constant.

Simulation with the SRW Code

In order to verify the feasibility of this calibration method, and provide comparative data of the experimental result, a simulation study has been done using SRW code.

SRW is a wave optics simulation code that can take the actual wave front of the light emitted by a filament like source in the bending magnet and propagete it. SRW can select a defined wavelength X-ray to do simulation research. In this article, we use SRW to study the novel PSF calibration method. The limitation is that this simulation study only calculate the PSF on the scintillator, this do not contain the PSF of the whole imaging system.

Optical arrangement in quasi-monochromatic X-ray pinhole camera simulation with SRW is show in Fig. 3. In the

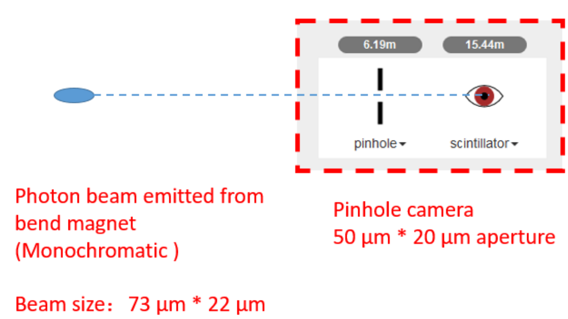

Figure 3: Optical arrangement in quasi-monochromatic X-ray pinhole camera simulation with SRW.

simulation process, horizontal beam size was set to 73 μm and vertical beam size was set to 22 μm.

According to the principle of the variable wavelength calibration method, during the calibration, the angle of the crystal will be changed to select different wavelength. The

ISBN: 978-3-95450-184-7 doi:10.18429/JACoW-IPAC2018-THPML070

problem is that the value of the wavelength is hard to know in the experiment. Spectrum is a very useful tool that can be used to characterize the intensity distribution of each wavelength of synchrotron light. The intensity value can be obtained from the images of different wavelength. In order to improve the result of the fitting, the range of the selected energy should cover the critical energy. The spectrum that of the photon beam without any filter is shown in Fig. 2, the critical energy is around 25.6 keV. Hence, during the simulation period, different photon energy is selected, the range is from 20 keV to 40 keV.

Figure 4 shows the image and corresponding profile obtained at the scintillator screen, when the photon energy is set to 26 keV.

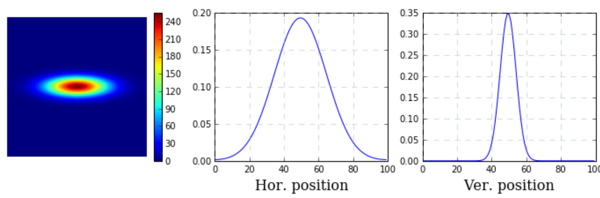

Figure 4: Image and corresponding profile obtained at the scintillator screen, when the photon energy is set to 26 keV.

Using Gaussian fit to these profile curves, the imaging spot size can be obtained. When the photon energy is 26 keV, the diffraction width is 6.1 μm (for the vertical direction).

In order to realize the new calibration method, Eq. (1) can be changed to:

$$\sigma_{aper}^2 = \sigma_{img}^2 - (C_{mag}\sigma_{beam})^2 - \sigma_{diff}^2 \qquad (5)$$

In this simulation, the pinhole camera system is same, the only change thing is the wavelength. So, for the PSFs of the pinhole camera, only diffraction width is changed. The diffraction width can be calculated with Eq. (3), the imaging spot size can be calculated with fitting the profile curve, and the beam size is constant, the only unknown parameter is the geometric projection width. Hence, using Eq. (5), by varying the wavelength of the X-ray, the PSF can be derived.

Figure 5 shows the imaging spot size and corresponding photon energy in the SRW simulation.

Equation (3) shows that the diffraction width is proportional to the wavelength. So the results shown in Fig. 5 agree well with the theoretical formula.

The variation trend of the diffraction width and the geometric width, during the calibration, is shown as Table 1.

The results shown in the table shows that the calculated geometric width is also changed. There are two possible reason, one is that the formula to calculate the diffraction width is not very suitable; the other is that this width also contains the PSF introduced by the screen. In the experiment data, maybe also has this problem.

Fortunately, the change of the calculated geometric width is not very big. So we can use the method of finding approximate solutions for multiple equations to calculate the geometric projection width. This method can effectively reduce the error introduced in the measurement process. The geometric projection width of the pinhole camera PSFs is 32.0 μm. when the photon energy is 26 keV, the PSF on the scintillatoris 32.2 μm.

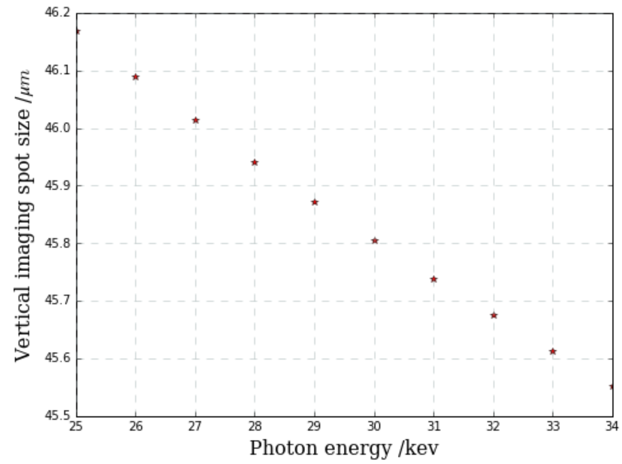

Figure 5: Imaging spot size and corresponding photon energy.

Table 1: The Variation Trend of the Diffraction Width and the Geometric Width

Photon Energy keV	**Diffraction width** μm	**Geometric width** μm
25	6.3	32.3
26	6.1	32.2
27	5.9	32.1
28	5.6	32.0
29	5.5	31.9
30	5.3	31.8
31	5.1	31.7
32	4.9	31.6
33	4.8	31.5
24	4.6	31.4

CONCLUSION

An X-ray quasi-monochromator has been installed at SSRF. Combined with this monochromator, the new X-ray pinhole camera is expected to calibrate the PSF under any beam conditions. In this article, a simulation study use SRW code is presented, the result shows that this method is able to realize the novel calibration method. This simulation results also can be used to verify the experiment data.

ISBN: 978-3-95450-184-7 doi:10.18429/JACoW-IPAC2018-THPML070

REFERENCES

[1] A. H. Lumpkin, B. X. Yang, C. Y. Yao *et al.*, " X-ray Imaging of the APS Storage Ring Beam Stability Effects: From the Alaskan Earthquake to Undulator Field Changes", in*Proc. Particle Accelerator Conf. (PAC'03)*, Portland, OR, USA, May 2003, pp. 2423–2425.

[2] M. J. Boland and M.Spencer, "Vertical Beam Profile Measurement and Analysis with an X-ray Pinhole", in *Proc. 11th European Particle Accelerator Conf. (EPAC'08)*, Genoa, Italy, Jun. 2008, pp. 1059–1061.

[3] J. C. Bergstrom and J. M. Vog, "The X-ray diagnostic beamline at the Canadian Light Source", *Nuclear Instruments and Methods in Physics Research A*, vol. 578, nos. 2-3, pp. 441–457, 2008.

[4] C. A. Thomas and G. Rehm, "Fast Pinhole Camera for Optimization of Top up Injection", in *Proc. 2008 Beam Instrumentation Workshop (BIW'08)*, Lake Tahoe, CA, USA, May 2008, pp. 279–281.

[5] G. Q. Huang, J. Chen, Z. C. Chen *et al.*, "X-ray pinhole camera system design for SSRF storage ring", *Nuclear Techniques*, vol. 33, no. 11, pp. 806–809, 2010.

[6] Y .B. Leng, G. Q. Huang, M .Z Zhang *et al.*, "The beam-based calibration of an X-ray pinhole camera at SSRF", *Chin. Phys. C*, vol. 36, p. 80, 2012.

[7] B. Gao, Y. B. Leng, H. J. Chen *et al.*, "Upgrade of the X-ray pinhole camera at SSRF", *Nuclear Science and Techniques*, to be published.

[8] O. Chubar and P. Elleaume, "Accurate and Efficient Computation of Synchrotron Radiation in the Near Field Region", in *Proc. 6th European Particle Accelerator Conf. (EPAC'98)*, Stockholm, Sweden, Jun. 1998. paper THP01G, pp.1177–1179.

[9] `https://www.britannica.com/science/spectroscopy/Energy-states-of-real-diatomic-molecules$\#$ref80642`

[10] Z. C. Chen, Y. B. Leng, J. Chen *et al.*, "Point spread function study of X-ray pinhole camera in SSRF", in *Proc. 4th Int. Particle Accelerator Conf. (IPAC'13)*, Shanghai, China, May 2013, paper MOPME053, pp. 592–594.